PHYSICAL REVIEW B, VOLUME 63, 035407

Kinetic Monte Carlo simulation of nucleation on patterned substrates

L. Nurminen, A. Kuronen, and K. Kaski

Helsinki University of Technology, Laboratory of Computational Engineering, P.O. Box 9400, FIN-02015 HUT, Finland

(Received 9 June 2000; revised manuscript received 18 August 2000; published 29 December 2000)

The effects of a patterned substrate on island nucleation are investigated using kinetic Monte Carlo simulations. Two different models are formulated by incorporating an inhomogeneous energy surface into the basic solid-on-solid model of epitaxial growth to describe surface diffusion and consequent island nucleation on a patterned substrate. These models are related to two examples of real systems in which preferential nucleation at specific sites is encountered. Growth on a patterned substrate produces quite uniformly sized islands, which are are found to order into regular arrays displaying the periodicity of the underlying substrate. Confinement due to the patterned substrate is observed to be strongly dependent on the growth conditions. We demonstrate that there exists an optimal set of growth conditions determined by the length scale of the substrate pattern. In addition, the influence of the patterned substrate on the process of Ostwald ripening is discussed.

DOI: 10.1103/PhysRevB.63.035407 PACS number(s): 79.60.Jv, 81.15.Aa, 02.70.Rr

I. INTRODUCTION

Much of the recent interest in studies of metallic and semiconductor systems has focused on atomic scale structures, due to their great potential for numerous technological applications.[1] For example, spontaneous self-organization of islands in heteroepitaxial thin-film growth has been utilized to manufacture semiconductor *quantum dots*. These three-dimensional structures, where electrons are confined to a nanometer scale in all three dimensions, have interesting optical properties. The fabrication of actual device structures is, however, problematic, since a large number of uniformly shaped and sized islands is required.

In the case of heterostructures, different properties of component materials can offer a way to grow a spatially ordered arrangement of islands with an improved size uniformity.[2] For example, quantum dot superlattices, which consist of several layers of different materials obtained by alternating growth of, e.g., GaAs and InAs, yield a structure with strained layers of InAs islands embedded in GaAs. The fascinating feature of this structure is that the islands tend to nucleate directly on top of the buried islands. This leads to a narrow island size distribution.[3–5] The vertical correlation in island positions is explained by the effect of strain on the surface caused by the underlying buried islands. This strain changes the activation energies of the diffusion of adatoms deposited on the strained surface, and thereby affects the nucleation of islands in the topmost layer.

In some heteroepitaxial systems strain due to lattice mismatch is relieved by the spontaneous formation of domains separated by a regular network of dislocations.[6] One example is a system of 2 ML of Ag deposited on Pt(111),[7,8] where dislocations constitute effective repulsive barriers for the diffusing adatoms on the surface, confining the adatoms to the domains. Consequently, nucleation on top of the dislocation network produces ordered arrays of rather uniformly sized submonolayer islands, most of which are located in spaces between dislocations.

In this work, we concentrate on the initial stages of growth, i.e., on the growth of two-dimensional islands that are formed in the submonolayer regime or *platelets*. The objective is to examine mechanisms that lead to spatially ordered nucleation and consequently to a narrow island size distribution. In this study we present two different models, motivated by the examples above. These are used to study qualitatively how the spatial variation in diffusion activation energy affects island nucleation.

This paper is organized as follows. In Sec. II we give details about the model systems and the simulation setup. In Sec. III we discuss our results. Finally, in Sec. IV we give a summary and concluding remarks.

II. SIMULATION MODEL

A. Diffusion model

In this study the kinetic Monte Carlo (KMC)[9,10] method is applied to investigate the time evolution of surface growth. The KMC method is based on a solid-on-solid[11] model of epitaxial growth, which assumes a simple cubic lattice structure with neither vacancies nor overhangs. The basic processes included in the model are *deposition of adatoms* and subsequent *surface diffusion*. The process of desorption has been omitted from the model since it is negligible under usual growth conditions of molecular beam epitaxy, which is commonly used in growing atomic scale structures. Thus the fractional surface coverage is given by $\Theta = Ft$, where F is the constant deposition rate of atoms in ML/s, and t is the physical time. The deposition of adatoms takes place onto an initially flat substrate. In the simulations a deposition site is first selected at random, and then a search is carried out within a square of fixed linear size of $2R_i+1$, centered upon the selected site. The site with a maximum number of lateral nearest neighbors is chosen as the deposition site.

The diffusion rate of a single adatom is defined as the probability of a diffusion jump per unit time, and it is given by the Arrhenius-type expression

$$k(E,T) = k_0 \exp(-E/k_B T), \tag{1}$$

where E is the activation energy, T is the substrate temperature, and k_B is the Boltzmann constant. The prefactor k_0 corresponds to the frequency of atomic vibrations, and it is

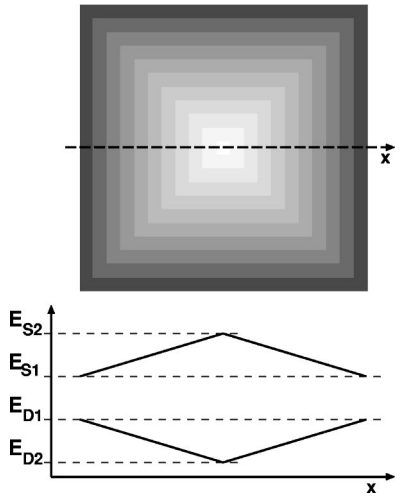

FIG. 1. Variation of the diffusion activation energies inside a single domain on the patterned substrate (schematic). The size of a single domain is 22×22 lattice sites, thus the whole substrate consists of 16×16 of these domains. The lower part of the figure shows the corresponding variations of the simulation model parameters E_S (model A) and E_D (model B) when traversing through the cross section of the domain as indicated in the upper figure.

assigned the value $k_0=2k_BT/h$,[12] where h is the Planck constant. In the basic model, the activation energy E comprises a substrate term E_S, and a contribution from each occupied lateral nearest neighbor atom, E_N,

$$E=E_S+nE_N, \tag{2}$$

where $n=0-4$ is the number of occupied lateral nearest neighbors at the *initial* site. In this basic model of diffusion, the adatom lands with equal probability to any of the four neighboring sites.

B. Patterned substrate

The purpose of this study is to build a simple model which captures the salient features of island nucleation on an inhomogeneous substrate. The patterned substrate is incorporated into the basic diffusion model described above by dividing the lattice into square-shaped domains of size $l\times l$. The square geometry is adopted for simplicity and to speed up the computation. The energy barriers for diffusion are varied within the domain structure in two ways (see Fig. 1).

(1) (Model A) The parameter E_S is let to vary piecewise linearly as a function of the lateral position of the adatom on the surface. The total barrier for diffusion is given by $E_A=E_S(x,y)+nE_N$.

(2) (Model B) An additional diffusion barrier E_D is introduced for the diffusion jumps directed toward the domain boundaries. The strength of the additional barrier is determined by the distance of the adatom from the boundary. The total barrier for diffusion is given by $E_B=E_S+nE_N+E_D$, where E_D depends on both the hop direction and the lateral position of the adatom on the surface.

Similar models are used in studies of tracer diffusion in disordered lattices to describe the energetic disorder experienced by the diffusing particle.[13,14] In the random-trapping model the binding energy of the particle varies from site to site (corresponding to our model A), while in the random-hopping model the saddle point energy between adjacent sites varies (model B in this work).

Of the systems described above the vertically correlated quantum dot superlattices serve as an experimental motivation for the model A. As explained in Sec. I, surface diffusion of adatoms and subsequent island nucleation in these systems are affected by the spatial bias that arises from the strain at the surface due to buried islands. The process of island nucleation is a complex issue, therefore a detailed analysis of a specific system would require much more detailed models and careful fitting of the parameters. However, in this work, we wish to examine the origin of possible mechanisms that lead to spatially ordered nucleation through the variation of diffusion activation energies. Model A describes a situation in which the energy surface seen by the diffusing adatom is spatially biased by some underlying structure of the substrate (e.g., buried islands).

Motivation for Model B, in turn, is based on the experimental system of Ag/2 ML Ag/Pt(111) heteroepitaxy. In this case, the substrate is patterned with a regular network of dislocations which act repulsively towards the diffusing adatoms.[6,8,15] In model B, we have included an additional, hop-direction-dependent diffusion barrier E_D, to describe the long-range repulsive adatom-dislocation interaction. It should be noted that such a barrier does not affect only the jumps that cross the domain boundaries but each adatom experiences a repulsion from all the boundaries which are within half the lateral size of a domain from the adatom.

The simulations presented in this work were carried out on a square lattice of size 352×352, with periodic boundary conditions. The domain size was selected to be 22×22, thus introducing an underlying superstructure of 16×16 square domains into the system. The values $E_S=0.75$ eV and $E_N=0.18$ eV were used for parameters describing the substrate and nearest-neighbor binding energies, respectively. These values were previously used to model qualitatively the effect of reentrant layer-by-layer growth observed for Pt(111) homoepitaxy.[16]

For model A, the variation of the substrate binding energy E_S inside each domain was chosen by performing some preliminary simulations. The values $E_{S1}=0.65$ eV and $E_{S2}=0.85$ eV (see Fig. 1) produced an effect which was clear but not artificially strong. The effect of varying these values was also examined (see Sec. III B). In the case of model B, the order of magnitude of the additional diffusion barrier, E_D, need not to be very large because it has been shown[17] that even a small increase in the diffusion barrier is feasible to lead to substantial changes in diffusivity. This is because adatoms have to make several jumps in an unfavorable direction to cross a dislocation. Based on this information, the values $E_{D1}=0.02$ eV and $E_{D2}=0$ eV were used for the maximum and minimum values of the additional barrier, respectively (see Fig. 1).

The deposition rate F was 0.0033 ML/s, and the value $R_i=1$ was used for the incorporation radius as in Ref. 16. These parameters are used in the simulations presented in

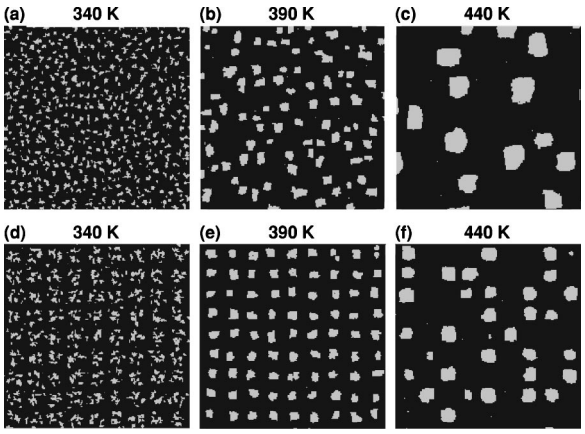

FIG. 2. Island morphologies obtained at three different temperatures (from left, 340, 390, and 440 K) for the homogeneous substrate (a)–(c), and for the patterned substrate (model B) (d)–(f). 200×200 surface sections of the whole system (352×352) are shown. The coverage is 15%. Dark areas designate the substrate and light areas the first layer of adatoms.

this study unless stated otherwise. The temperature range of interest was determined by the behavior of the system. We found that in the simulations for the chosen parameter set the effect of patterned substrate on nucleation was most pronounced for the temperature range $T=360$–420 K.

III. RESULTS AND DISCUSSION

In our computational experiments thin film growth on solid substrates is initiated by the nucleation of small two-dimensional (2D) islands, which can then serve as templates for the development of larger 3D islands. Although our model allows three-dimensional growth, we do not expect it to be described realistically. This does not, however, pose any problems because all the results presented here are for systems that have reached an adatom coverage of up to 15% in the simulations, at which point the islands are still purely two dimensional. In this study, we are interested in the development of surface morphology and in the size distribution of nucleated islands. For sufficient statistics for the results, we have taken ensemble averages over 50 simulation runs.

A. Effect of patterned substrate

Figures 2(a)–2(c) show examples of island morphologies at three different temperatures for samples grown on a homogeneous substrate. In agreement with the theory of submonolayer epitaxy, the 2D islands are randomly distributed on the surface, and the average island separation corresponds to the average diffusion length of adatoms. Since diffusion is a thermally activated process, increasing the temperature is expected to lead to a large average island size and separation between them, as we also observe.

When the substrate is patterned, it has a strong effect on both the positioning and the average size of the growing islands, as indicated by Figs. 2(d)–2(f). In both patterned substrate models the inhomogeneity in the activation energies of diffusion produces a net flow of adatoms toward the centers of the domains. Consequently, the domain centers act as preferential nucleation sites.

As for the arrangement of islands on the surface we have found it to be strongly dependent on the growth temperature. At low temperatures [Fig. 2(d)], the average diffusion length is so short that several small islands nucleate within each domain. The island density is highest near the domain centers. At intermediate temperatures [Fig. 2(e)], the average diffusion length corresponds to the lateral size of the domains, thus the adatoms are able to visit all parts of the domain into which they were deposited. This leads to the nucleation of a single island within each domain. The domains act as equally large capture areas for the islands, thus we also observe an enhanced size uniformity. When the temperature is further increased [Fig. 2(f)], adatom diffusion across the domain boundaries becomes activated. As a result, some of the domains are left empty when smaller islands dissociate, and the adatoms join surrounding larger islands. This corresponds to 2D Ostwald ripening,[6,18] although the process is affected by the patterned substrate. Ostwald ripening and the high-temperature behavior of the systems are discussed in more detail below (see Sec. II C).

Figure 4(a) shows the average island size $\langle s\rangle$, plotted as a function of temperature for the homogeneous substrate and for both patterned substrate models A and B. Here $\langle\ \rangle$ denotes the ensemble average, i.e., the average over many simulation runs. As inspection of the island morphologies (Fig. 2) already indicated, the patterned substrate has a strong effect on the average island size. For samples grown on a homogeneous substrate, the islands grow smoothly with increasing temperature. In the case of a patterned substrate, we observe that the average island size stays approximately constant ($s\approx73$) for temperatures ranging from 370 to 400 K. Thus the islands on a patterned substrate are less sensitive to small changes in the growth conditions, which is significant because precise control over the island characteristics is required for technological applications of nanostructures.

In addition to the average island size, we are also interested in the variations the islands exhibit in their size. These variations are measured by calculating the island size distribution, $N(s,t)=N_s(t)$, which is defined as the areal density of islands composed of s atoms ($s>1$) at time t. Figure 3 shows the development of the island size distribution as a function of temperature for the homogeneous substrate and the patterned substrate of model A. The corresponding curves for model B have not been plotted, because they turned out to be very similar to those for model A. The differences between these two models are discussed later in the text (see Secs. III B and III C).

We also point out that the form of the island size distribution curves is in good agreement with the behavior observed from the lattice pictures (Fig. 2). At very low temperatures, the curves for both the homogeneous and the patterned substrate exhibit a high and narrow peak at small values of s. For islands grown on a homogeneous substrate, the size distribution broadens smoothly with increasing temperature. For the patterned substrate, an additional maximum appears around $s=70$ at temperature $T=360$ K. This is caused by the coalescence of several small, neighboring is-

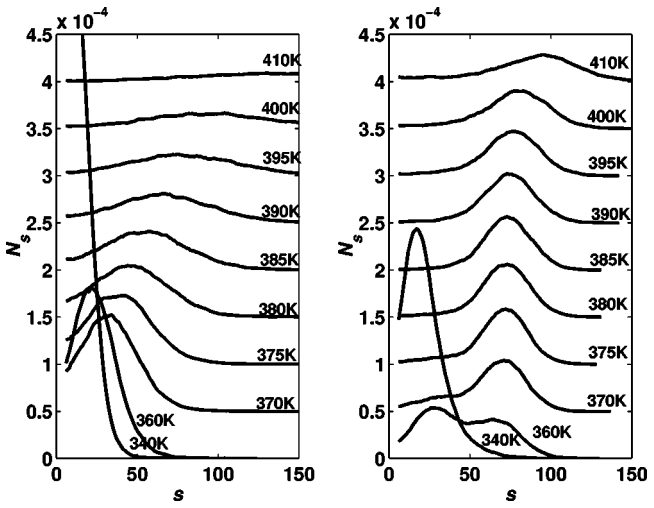

FIG. 3. Island size distributions as a function of temperature for the system with homogeneous substrate (on the left) and with the patterned substrate (model A) (on the right). The coverage is 15%. The horizontal axis is the number of particles in the island and the vertical axis is in units of islands per lattice site. Curves for temperatures of 370–410 K have been shifted by 5×10^{-5} relative to the preceding curve.

lands within each domain. For the temperature range $T=370$–400 K, the island size distribution stays approximately constant due to the confinement effect caused by the substrate pattern. Each domain contains a single island which consists of $s=73$ atoms on average (when the coverage is 15% and the domain size is 22×22). When the temperature is increased above $T=400$ K, the distribution begins to broaden, and the maximum shifts toward higher values of s as a consequence of interdomain diffusion.

Hence we conclude that there exists an optimal growth temperature at which nucleation on a patterned substrate results in high spatial ordering and enhanced size uniformity of the islands. The optimal growth temperature can be measured by monitoring the relative width of the island size distribution w, defined as $w=\sigma/\langle s\rangle$, where $\sigma=\sqrt{\langle s^2\rangle-\langle s\rangle^2}$ is the standard deviation of the island size distribution, and $\langle s\rangle$ is the average island size. The smaller the value of w is, the smaller the fluctuations in island sizes are. Thus the optimal growth temperature can be identified by locating the point at which w reaches its minimum value.

Figure 4(b) shows w as a function of temperature for the homogeneous substrate and for the patterned substrate models A and B. At low temperatures, the values of w are higher for the patterned substrates, because the coalescence of neighboring islands near the domain centers results in larger fluctuations in island sizes. However, in the temperature range from 360 to 420 K, the decrease in the relative width of the size distribution shows that the islands on the patterned substrates are clearly more uniformly sized than the islands on the homogeneous substrate. Moreover, we observe that the curve for w has a local minimum at approximately 390 K in the case of model B, and for model A the minimum is reached at a slightly lower temperature. At this temperature the average diffusion length is equal to the average island separation, which is determined by the size of the do-

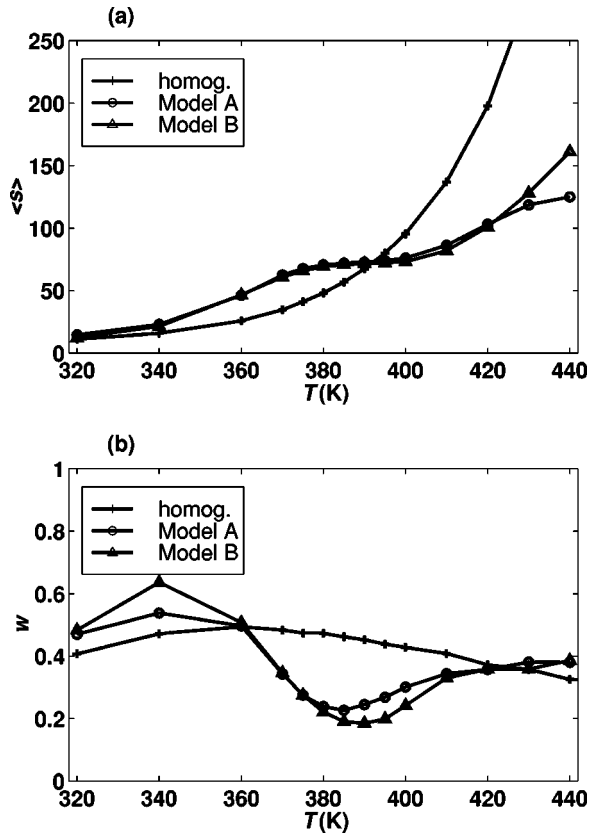

FIG. 4. (a) Average island size and (b) relative width of the island size distribution as a function of temperature for the homogeneous substrate, model A, and model B. The coverage is 15%.

mains. The domains act as equally large capture areas for the islands; therefore, the small fluctuations in island sizes are caused mainly by the randomness in the deposition process. At high temperatures, the relative width of the size distribution increases again when diffusion across the domain boundaries results in the formation of larger and smaller islands, as already mentioned. It should be noted that essentially the same behavior is observed if the deposition rate is varied while keeping the temperature constant.[19]

We now relate our two models with the two experimental cases discussed in Sec. I. First we take the case of the vertical sequence of the quantum dot superlattice, which we expected to be partially described with model A. Although in this case there is experimental evidence for the vertical correlation of quantum dot positions in superlattices,[4,20] the exact mechanism of the preferred nucleation is not clear. It is assumed that the nucleation of adatoms forming the quantum dot takes places at the minima of the strain energy caused by the underlying dot.[21,20] However, currently the effect of strain on adatom diffusion on semiconductor surfaces is not well understood.[22] It should be noted that in this study we have only concentrated on the initial stages of island growth, while experiments have been conducted to the full three-dimensional layered heterostructures without paying attention to the initial stages of growth.

As for the relation of the model B with the second experimental case, i.e., the system of metallic heterostructure, it should be noted that the number of experimental measure-

ments of diffusion and nucleation on an inhomogeneous substrate is currently very limited. Nonetheless, we can make qualitative comparisons to the results of Brune and coworkers, [7,8] who studied the system of Ag/2-ML Ag/Pt(111). In our simulations, we have included the long-range repulsive adatom-dislocation interaction that in Refs. 7 and 8 was proposed to be the key property leading to confined nucleation. When comparing the lattice pictures obtained from our simulations [Figs. 2(d)–2(f)] to the series of scanning tunneling microscopy images in Ref. 8, we find that our results agree very well with the experiments. The periodicity of the dislocation network is transferred to a highly ordered two-dimensional island superlattice for a narrow temperature range. At temperatures below this range, several islands nucleate within each unit cell, and at higher temperatures the island density drops when the adatoms are able to overcome the repulsive barriers due to dislocations. Our simulations reproduce this experimentally observed behavior at various temperatures.

B. Effect of model parameters

In order to gain insight into the differences in the behavior of models A and B, effects of varying the model parameters were studied. The strength of the substrate pattern is determined by the difference between the parameters E_{S1} and E_{S2} for model A, and E_{D1} and E_{D2} for model B. Figure 5(a) shows the results of simulations for model A, and Fig. 5(b) results for model B, using three different strengths of the substrate pattern in each case.

For model A, using a smaller value of E_{S1} and a larger value of E_{S2} extends the temperature range in which the confinement effect of the patterned substrate results in a narrow distribution of island sizes. First we observe that the behavior of the system is unaffected at temperatures below 380 K. This is due to the fact that at these temperatures the average diffusion length is so short that the net movement of adatoms is not affected by small changes in the diffusion activation energies.

In the case of model B, the strength of the substrate pattern is determined by the maximum value of the additional diffusion barrier, E_{D1}. As expected, a larger value of E_{D1} produces a strong confinement. In this case, however, the behavior of the system is influenced in the whole temperature range from 320 to 440 K. This is explained by the hop-direction dependence of the additional diffusion barrier, E_D. A larger repulsion from the domain boundaries drives the adatoms more effectively toward the centers of the domains, even at low temperatures. This leads to the coalescence of several small islands, and to a consequent increase in the relative width of the size distribution.

C. High-temperature behavior and Ostwald ripening

We have also studied the high-temperature behavior of the model systems and the process of 2D Ostwald ripening in more detail. On a homogeneous substrate, the average island size grows with increasing temperature until the average diffusion length becomes comparable to the size of the simulation system. The process of 2D Ostwald ripening leads to

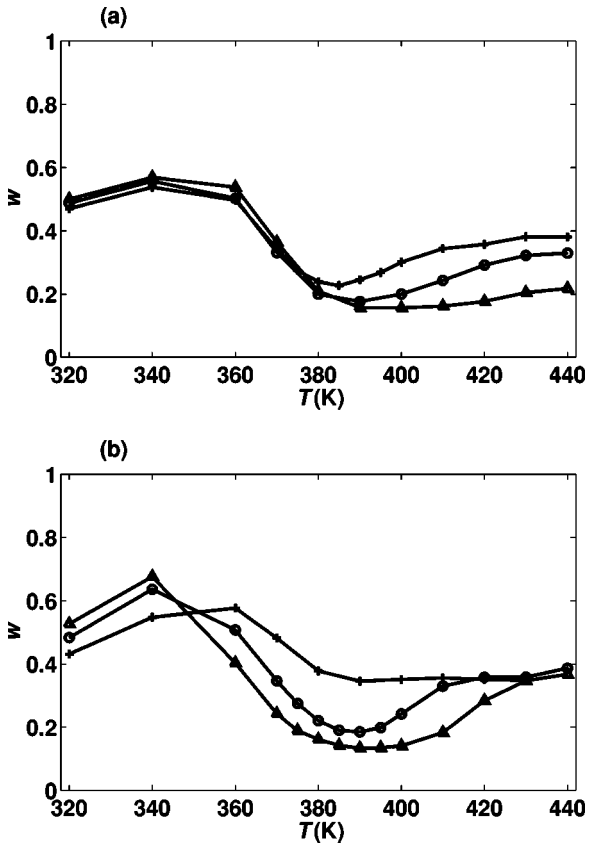

FIG. 5. Effect of varying the strength of the substrate pattern. The relative width of the island size distribution is shown (a) for model A using the parameter values $\{E_{S1},E_{S2}\}=\{0.65,0.85\}$ eV (+), $\{0.60,0.90\}$ eV (○), and $\{0.55,0.95\}$ eV (△); and (b) for model B using the parameter values $\{E_{D1},E_{D2}\}=\{0.01,0\}$ eV (+), $\{0.02,0\}$ eV (○), and $\{0.03,0\}$ eV (△).

similar behavior if we follow the development of the adlayer after the deposition has been stopped: small islands dissociate in favor of larger ones until the simulation system consists of a single large cluster. At very high temperatures, diffusion is so fast in the time scale of deposition that Ostwald ripening takes place simultaneously with growth.

In contrast, on a patterned substrate we observe a different kind of post-deposition behavior of the adlayer. Figures 6(a)–6(c) and 6(d)–6(f) show the post-deposition development for models A and B, respectively. The initial configurations [Figs. 6(a) and 6(d)] were created by random deposition of 10% coverage of adatoms. In both cases, an ordered array of 2D islands forms quickly after the deposition had been stopped [Figs. 6(b) and 6(e)]. In the case of model A, further diffusion does not change the arrangement of islands notably [Fig. 6(c)]. We observe the same behavior when the growth temperature is sufficiently high. In Fig. 7 we show the relative width of the island size distribution for model A as a function of temperature. The distribution becomes increasingly narrow until the system reaches a stable state around 500 K. Thus the patterned substrate not only enhances the spatial ordering and size uniformity of the islands, but also increases the stability of the configuration. In the case of model B, the process of Ostwald ripening is not

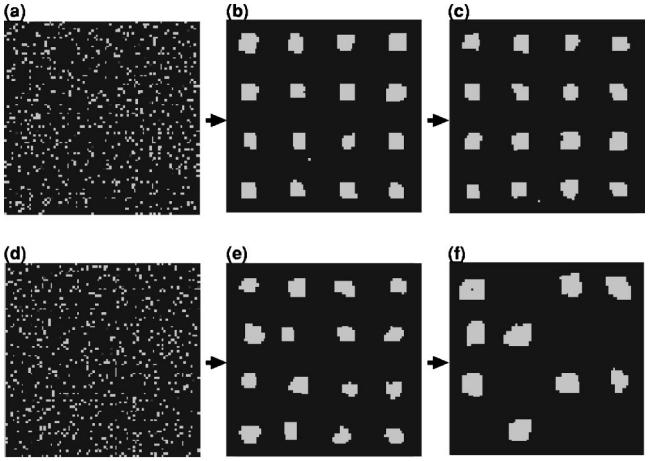

FIG. 6. Post-deposition development of surface configurations for model A (a)–(c) and for model B (d)–(f). The initial configurations (a) and (d) were obtained by random deposition of adatoms to the coverage of 10%. The temperature is 400 K. 88×88 surface sections of the whole system (352×352) are shown.

completely suppressed by the inhomogeneous energy surface of the substrate. Even though the islands first order into a regular array, further diffusion leads to the dissociation of smaller islands in favor of larger ones as can be seen from Fig. 6(f). However, this process is considerably slower than on a homogeneous substrate.

The differences in the behavior between models A and B can be explained by considering the total diffusion rate of an adatom in different positions on the substrate. In the case of model A, the closer to the domain centers the adatoms are, the more tightly they are bound to the substrate. In other words, diffusion is slow in the center areas of the domains and fast near the boundaries of domains, and consequently, the energetically most favorable configuration is a single island within each domain. In the case of model B, the hop-direction dependence of the additional diffusion barriers produces an effective change in the direction of the net movement of adatoms, but the change in the total diffusion rate is very small. Therefore, a single island forms within each domain during the initial nucleation process (under favorable growth conditions), but afterward Ostwald ripening leads to the dissociation of smaller islands in favor of larger ones.

IV. CONCLUSION

In summary, we conclude that periodic inhomogeneity in the activation energy for adatom diffusion significantly affects the nucleation process on the substrate. We have demonstrated that nanoscale patterning of the substrate can lead to the formation of an ordered array of 2D islands with a narrow size distribution. Our simulation results also indicate that the confinement effect of the patterned substrate is strong in a narrow temperature range. The length scale of the substrate pattern determines the optimal growth temperature at which the fluctuations in island sizes reach a minimum value. Alternatively, the particle flux can be tuned to find the most optimal growth conditions. We find that the results of our simulations are in good qualitative agreement with experimental observations.

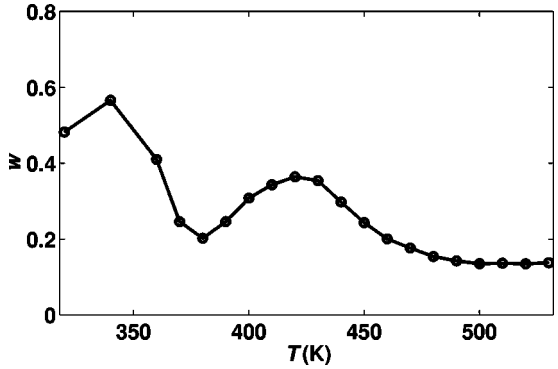

FIG. 7. High-temperature behavior of the relative width of the size distribution for the patterned substrate model A with $E_N = 0.16$ eV.

In order to compare with previous simulation studies, we refer to the work by Lee and Barabási[23] who studied island growth on a sample patterned with an ordered impurity array using various deposition rates. Our results are similar to theirs in indicating that the spatial ordering and size distribution of the islands are enhanced if the patterned substrate promotes preferential nucleation at specific sites. In our work, we have also demonstrated that different mechanisms can lead to periodic inhomogeneity in the diffusion activation energies. Thus we propose that substrate patterning could be used in various systems ranging from metals to semiconductor compounds to improve the quality of nanostructures produced in heteroepitaxy.

The models of this study were formulated on the basis of two examples of real systems in which diffusion is affected by the inhomogeneity of the substrate. In the current work, we have performed detailed simulations based on these atomistic models, and analyzed the effect of growth conditions and model parameters on the observed behavior. We conclude that diffusion and nucleation on an inhomogeneous substrate is a complex issue that offers many challenges for future studies.

Finally we note that strain is not *directly* included in the models presented in this study, although we propose that a patterned substrate could originate from strain induced effects. Strain acts as a self-limiting process in island growth as adatom detachment from larger islands is enhanced.[24] Thus the formation of large islands is suppressed, which leads to a narrower island size distribution. In future work, we plan to investigate this issue further by including elastic interactions directly into the diffusion model.

ACKNOWLEDGMENTS

The authors wish to thank Professor David P. Landau for helpful discussions. This work was supported by the Academy of Finland, project on Computational Research of Semiconductor Materials, Project No. 1169043 (Finnish Center of Excellence Program 2000-2005).

[1] D. Bimberg, M. Grundmann, and N. Ledentsov, *Quantum Dot Heterostructures* (Wiley, Chichester, 1999).
[2] M. Bartelt, A. Schmidt, J. Evans, and R. Hwang, Phys. Rev. Lett. **81**, 1901 (1998).
[3] J. Tersoff, C. Teichert, and M. Lagally, Phys. Rev. Lett. **76**, 1675 (1996).
[4] G. Springholz, V. Holy, M. Pincolits, and G. Bauer, Science **282**, 734 (1998).
[5] I. Kegel, T. H. Metzger, J. Peisl, J. Stangl, G. Bauer, and D. Smilgies, Phys. Rev. B **60**, 2516 (1999).
[6] H. Brune, Surf. Sci. Rep. **31**, 121 (1998).
[7] H. Brune, M. Giovannini, K. Bromann, and K. Kern, Nature (London) **394**, 451 (1998).
[8] K. Bromann, M. Giovannini, H. Brune, and K. Kern, Eur. Phys. J. D **9**, 25 (1999).
[9] M. Kotrla, Comput. Phys. Commun. **97**, 82 (1996).
[10] A. Levi and M. Kotrla, J. Phys.: Condens. Matter **9**, 299 (1997).
[11] J. D. Weeks and G. H. Gilmer, Adv. Chem. Phys. **40**, 157 (1979).
[12] P. Šmilauer and D. Vvedensky, Phys. Rev. B **52**, 14 263 (1995).
[13] Y. Limoge and J. L. Bocquet, Phys. Rev. Lett. **65**, 60 (1990).
[14] J. W. Haus and K. W. Kehr, Phys. Rep. **150**, 263 (1987).
[15] H. Brune, H. Röder, C. Boragno, and K. Kern, Phys. Rev. B **49**, 2997 (1994).
[16] P. Šmilauer, M. Wilby, and D. Vvedensky, Phys. Rev. B **47**, 4119 (1993).
[17] H. Brune *et al.*, Phys. Rev. B **52**, 14 380 (1995).
[18] N. C. Bartelt, W. Theis, and R. M. Tromp, Phys. Rev. B **54**, 11 741 (1996).
[19] Nucleation is governed by the ratio (D/F), where $D=k_0 \exp(-E_S/k_BT)$ is the monomer diffusion rate and F is the deposition rate. Therefore, lowering the deposition rate has essentially the same effect as raising the temperature. Additional simulations were performed to confirm this.
[20] V. Holý, G. Springholz, M. Pinczolits, and G. Bauer, Phys. Rev. Lett. **83**, 356 (1999).
[21] Q. Xie, A. Madhukar, P. Chen, and N. P. Kobayashi, Phys. Rev. Lett. **75**, 2542 (1995).
[22] E. Zoethout, O. Gürlü, H. J. W. Zandvliet, and B. Poelsema, Surf. Sci. **452**, 247 (2000).
[23] C. Lee and A.-L. Barabási, Appl. Phys. Lett. **73**, 2651 (1998).
[24] C. Ratsch, M. D. Nelson, and A. Zangwill, Phys. Rev. B **50**, 14 489 (1994).